

VIII. PLASMA ELECTRONICS*

Prof. L. D. Smullin	P. H. Edmonds	M. A. Lieberman
Prof. H. A. Haus	S. A. Evans	M. Lind
Prof. A. Bers	T. J. Fessenden	J. D. Mills
Prof. W. D. Getty	R. W. Flynn	A. A. Offenberger
Prof. P. Penfield, Jr.	F. Gardiol	K. C. Papadopoulos
Prof. D. J. Rose	E. T. Gerry	R. R. Parker
Prof. T. H. Dupree	J. N. Hamawi	L. M. Petrie, Jr.
Prof. L. M. Lidsky	R. Hancox	C. S. Ribbeck
Prof. E. P. Gyftopoulos	C-F. G. Hsi	J. A. Ross
R. R. Bartsch	H. Y. Hsieh	H. M. Schneider
R. J. Briggs	G. I. Kachen, Jr.	P. S. Spangler
T. S. Brown	C. A. Kapetanakos	E. Thompson
J. F. Clarke	B. R. Kusse	C. E. Wagner
J. A. Davis	S. H. Kyong	R. N. Wallace
F. E. Dunn		J. C. Woo

A. BEAM PLASMA DISCHARGE: SYSTEM C

1. Modifications of the Vacuum System

The vacuum system of System C has been modified in order to obtain a lower base pressure and to reduce wall outgassing by the plasma. A 400-liter/sec VacIon pump was installed in place of the oil diffusion pump. All of the large O-ring seals were replaced by copper gaskets and Conflat flanges, and the remaining O-rings were replaced by Viton O-rings. A heating tape was wrapped around the vacuum tube, and the tube and tape were then wrapped with an asbestos paper blanket. Maximum bake-out temperatures of 100-120°C can be obtained with this arrangement. The minimum pressure obtained thus far is 2×10^{-8} torr.

To avoid overloading the VacIon pump with hydrogen when the operating pressure is $\sim 10^{-5}$ torr, we installed a pulsed valve to admit the gas. The pressure rise time is 20 msec, and the best pressure decay time observed thus far is 80 msec for hydrogen. This arrangement gives a pumping speed of 440 liters per second for hydrogen, and an equivalent pumping speed of 160 liters per second for air in the 6-inch manifold above the pump. The pressure decay time limits our pulse repetition rate to a minimum of 1-2 seconds per pulse. The electron beam is triggered when the pressure reaches its maximum value. A peak pressure of 10^{-4} torr is readily attained without overloading the VacIon pump.

2. Experiments with the Rebuilt System C

An initial set of experiments was performed by injecting an electron beam from a magnetron injection gun of $\sim 10^{-5}$ perveance into hydrogen at pressures in the range

*This work was supported in part by the National Science Foundation (Grant GK-19); and in part by Purchase Order DDL BB-107 with Lincoln Laboratory, a center for research operated by Massachusetts Institute of Technology, with the support of the U. S. Air Force under Contract AF 19(628)-500.

(VIII. PLASMA ELECTRONICS)

5×10^{-6} – 5×10^{-4} torr. The beam voltage was varied from 4 kv to 20 kv, and had a duration of 700 μ sec. The confining magnetic mirror had a peak field strength of approximately 3000 gauss and a mirror ratio that could be varied from 2 to 5. The following properties of the plasma created by the resultant beam-plasma interaction were measured: (i) density, measured by means of a 93-Gc interferometer; (ii) transverse energy density, measured by means of a diamagnetic probe; (iii) total light emitted; and (iv) total x-ray intensity.

The most remarkable new result that was obtained was a pronounced decrease in the total light emitted by the plasma. During this decrease, which occurred soon after the initiation of the discharge, the diamagnetic probe signal either increased or remained approximately the same. This effect is illustrated in Fig. VIII-1 in which oscillograms of the diamagnetic probe, total light (detected by a Type 931A photomultiplier), and total x-ray signals are displayed for three beam voltages at a constant pressure of 7×10^{-5} torr. The x-ray detector was saturated under these operating conditions.

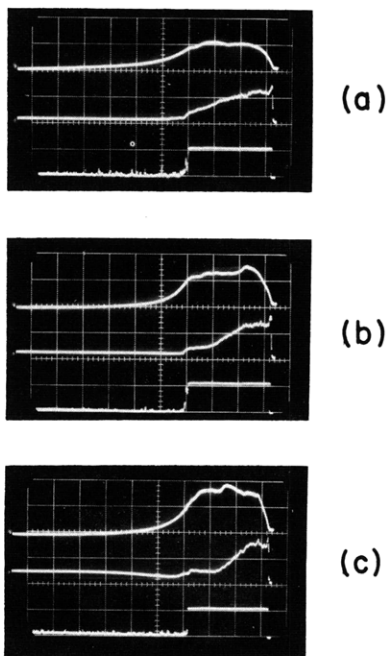


Fig. VIII-1. Oscillograms of diamagnetic probe, total light, and total x-ray signals. (a) $V_{\text{beam}} = 12$ kv. (b) $V_{\text{beam}} = 16$ kv. (c) $V_{\text{beam}} = 18$ kv. In each case, upper trace is the diamagnetic probe signal; middle trace, the photomultiplier signal; lower trace, the total x-ray signal; calibrations are the same. Time scale: 200 μ sec/cm.

The decrease in light may be due to 100 per cent ionization of the hydrogen gas. Interferometric measurements of the density under the conditions when this decrease of light takes place confirm that the plasma density remains approximately constant. This is also indicated by the diamagnetic probe signal (see Fig. VIII-1).

L. D. Smullin, W. D. Getty, R. R. Parker

B. COMPUTER DISPLAY SYSTEM FOR ANALYZING INSTABILITIES

A computer display system has been developed for analyzing instabilities in a plasma according to the mathematical criteria of Bers and Briggs.^{1, 2} The system uses the Electronics Systems Laboratory display console in conjunction with the Project MAC time-sharing system.

The user must provide a subroutine to the display program and must specify the dispersion relation for the physical system that he wishes to analyze. The display program requires a dispersion equation that is a polynomial in complex frequency, $\omega(\omega=\omega_r+j\omega_i)$, and complex wave number, $k(k=k_r+jk_i)$. Specifically, the coefficients of the powers of frequency and wave number are expressed in matrix form as follows:

$$\begin{array}{c}
 \omega^0 \quad \omega^1 \quad \dots \quad \omega^j \quad \dots \quad \omega^n \\
 \left[\begin{array}{cccccc}
 k^0 & a_{0,0} & a_{0,1} & \dots & a_{0,j} & \dots & a_{0,n} \\
 k^1 & a_{1,0} & a_{1,1} & \dots & a_{1,j} & \dots & a_{1,n} \\
 \vdots & \vdots & \vdots & & \vdots & & \vdots \\
 \vdots & \vdots & \vdots & & \vdots & & \vdots \\
 k^i & a_{i,0} & a_{i,1} & \dots & a_{i,j} & \dots & a_{i,n} \\
 \vdots & \vdots & \vdots & & \vdots & & \vdots \\
 \vdots & \vdots & \vdots & & \vdots & & \vdots \\
 k^m & a_{m,0} & a_{m,1} & \dots & a_{m,j} & \dots & a_{m,n}
 \end{array} \right]
 \end{array}$$

Thus, the coefficient of ω^j is

$$\sum_{i=0}^m (a_{i,j}) \cdot (k^i),$$

and the coefficient of k^i is

$$\sum_{j=0}^n (a_{i,j}) \cdot (\omega^j).$$

The user of this program is queried concerning the degrees of k and ω , the scaling of the axes, the ranges on the variables, and the choice of complex planes to be plotted (ω or k). As the user types the answers on the teletype, the program solves the equation and plots the data on the display. Then it returns to the beginning of the sequence of questions so that the parameters may be varied for another display.

Work continues toward providing aids to the user. These aids include rescaling of data without recalculation, incremental plotting, blanking of axes, and translation of data.

J. D. Mills

(VIII. PLASMA ELECTRONICS)

References

1. A. Bers and R. J. Briggs, Criteria for determining absolute instabilities and distinguishing between amplifying and evanescent waves, Quarterly Progress Report No. 71, Research Laboratory of Electronics, M.I.T., October 15, 1963, pp. 122-131.
2. A. Bers and J. D. Mills, Computer analysis and display of wave instabilities, Quarterly Progress Report No. 73, Research Laboratory of Electronics, M.I.T., April 15, 1964, pp. 85-86.

C. ELECTRON CYCLOTRON RESONANCE DISCHARGE*

Since the last quarterly report¹ the analysis of the x-rays emitted by ECRD has been continued. A 400-channel pulse-height analyzer, a sodium iodide scintillator, and a lead collimator were used. The collimator consists of two 1 1/2 inch lead walls that are placed 16 inches apart and that have 3/16 inch holes drilled through them for passage of x-rays. The scintillator is placed behind the second wall and inside a lead cylinder which has 2-inch lead walls. The collimator has an angular view of 4.4×10^{-4} steradians and views an area of approximately 2 cm^2 at the center of the experimental cavity.

A window that consisted of a sheet of 0.005-inch mylar stretched across a rubber "O" ring was constructed in the cavity. The collimator looked into the cavity through the mylar window.

Figure VIII-2 shows two typical x-ray spectra obtained by the pulse-height analyzer. The ordinate is the number of counts per channel of the analyzer and the abscissa is the energy of the detected photons, or equivalently the channel number. For these experiments, the analyzer was calibrated by using a Cs^{137} x-ray source so that a photon whose energy is between 298.5 keV and 300 keV falls into the 200th channel of the analyzer. These data were obtained from a discharge in hydrogen at pressures of 6×10^{-5} and 1.2×10^{-4} torr. For both experiments, adjustment of the magnet current to 40 amps placed the region of cyclotron resonance at the mid-plane of the cavity. The analyzer counted pulses for a two-minute period.

It is known² that if the electron distribution function is Maxwellian, the Bremsstrahlung intensity spectrum varies as $\frac{1}{E} e^{-E/T}$, where E is the energy of the photons, and T is the energy of the electrons. Thus, for sufficiently large E, the exponential factor dominates and the spectrum falls off as $e^{-E/T}$, which appears as a straight line on a logarithmic plot. Consequently, the dotted lines drawn through the data indicate the "temperature" of the high-energy tail of the electron distribution function.

*This work was supported in part by the U. S. Atomic Energy Commission (Contract AT(30-1)-3221).

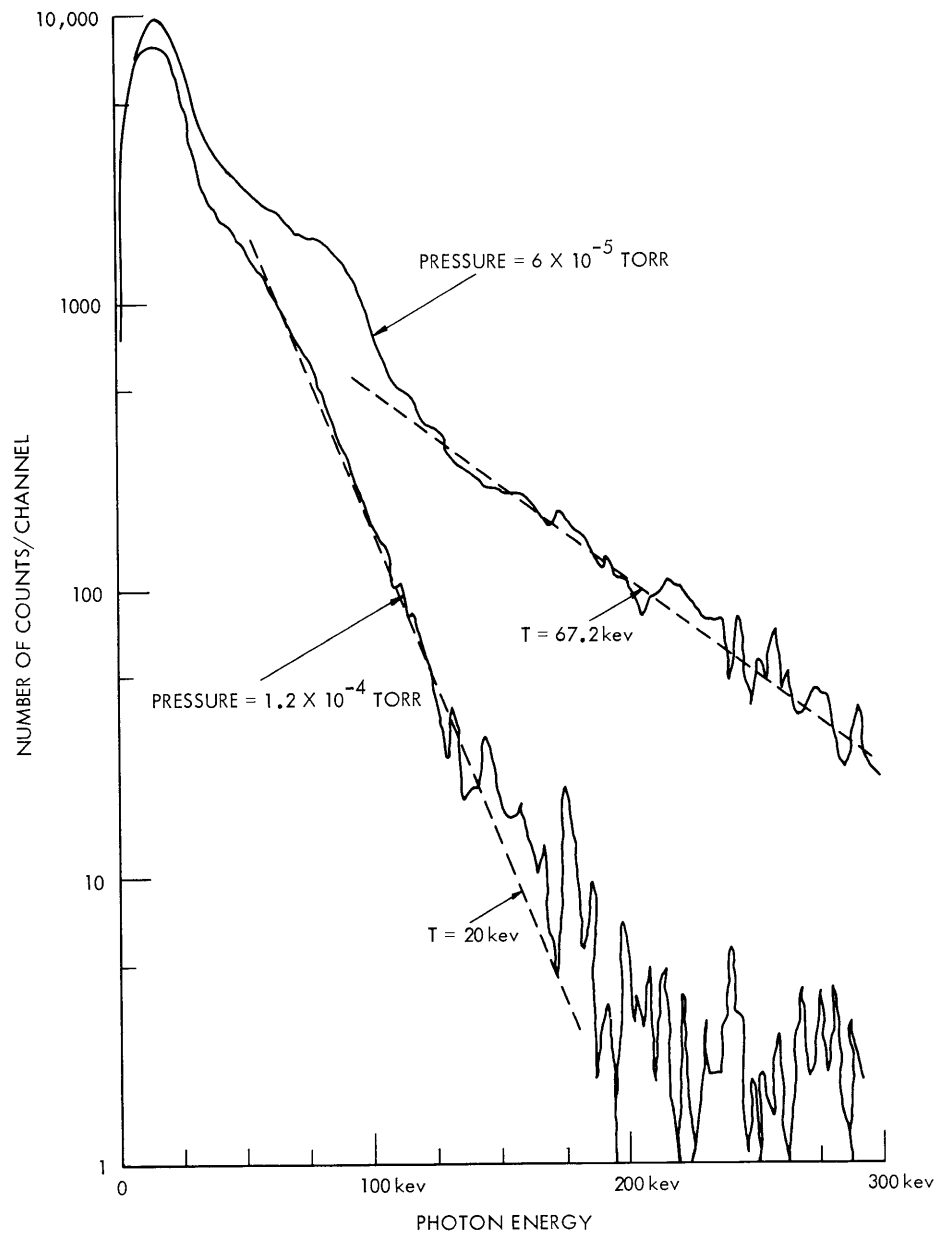


Fig. VIII-2. Two-minute counts of the x-ray energy spectra obtained from a discharge in hydrogen at pressures of 6×10^{-5} and 1.2×10^{-4} torr. Incident microwave power level, 100 kw peak; repetition rate, 1000 pulses/second; pulse-width, 1 μ sec; magnet current, 40 amps.

Many more experiments have been planned in which these techniques will be used to study the variation of the electron distribution function with pressure, incident microwave power, and magnetic field.

T. J. Fessenden

(VIII. PLASMA ELECTRONICS)

References

1. T. J. Fessenden, Quarterly Progress Report No. 74, Research Laboratory of Electronics, M. I. T., July 15, 1964, pp. 139-140.
2. L. Spitzer, Jr., Physics of Ionized Gases (Interscience Publishers, Inc., New York, 1956), p. 89.

D. ANOMALOUS SCATTERING OF LASER RADIATION FROM A PLASMA*

The work reported¹ in Quarterly Progress Report No. 73 has continued and, as a result of more detailed calculations, several previous conclusions have either been modified or discarded.

The experiment that we carried out in an attempt to observe Thomson scattering from plasma electrons has already been described.² Fifty joules of light at 6934 Å from a ruby laser was directed to intercept a DC plasma column, which had an electron density $\approx 10^{13}$ electrons cm^{-3} . Scattered radiation, after spectral analysis by a tunable 5 Å passband interference filter, was detected with a photomultiplier having an S.20 response.

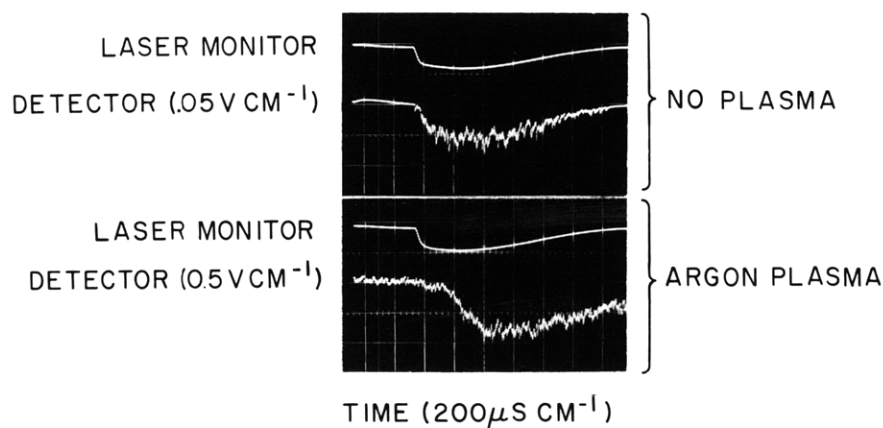


Fig. VIII-3. Oscilloscope traces showing typical delayed signals from the plasma. Upper trace shows the level of scattered radiation.

One set of data gave signals that could be interpreted as being due to Thomson scattering, whereas most of the signals were similar to those shown in Fig. VIII-3 and were delayed in time with respect to the laser monitor. (Note that the radiation

* This work was supported in part by the U. S. Atomic Energy Commission (Contract AT(30-1)-3285).

scattered from the walls of the vacuum chamber, etc. is synchronous with the input power; therefore, the delay that is observed in the lower trace is not attributable to the electronic equipment.) The amplitude of these delayed signals was constant over the spectral range (6940 Å-6600 Å) scanned by the filter. Furthermore, the radiation was found to be unpolarized by passing it through a sheet of polaroid film, whose optical axis could be varied with respect to the plane of polarization of the laser light. These properties are in marked contrast to radiation expected from Thomson scattering, which should be: (a) synchronous with the input radiation, (b) a Gaussian distribution in amplitude centered on the input wavelength for a Maxwell-Boltzmann distribution of plasma electrons, and (c) plane-polarized in the same sense as the input laser beam.

It has been suggested³ that these delayed signals appear as a result of photo-ionization by the laser beam of those excited neutral atoms in the plasma whose ionization potential is less than 1.79 ev. For example, the $n = 3$ level in hydrogen, where n is the principal quantum number, lies 1.51 ev below the continuum and can therefore be ionized by the 1.79-ev photons produced by the ruby laser operating at 6934 Å. The local increase in electron density, which results from this additional source of ionization, is accompanied by an increase in the rate of radiative recombination in the plasma. It is the continuum radiation emitted as a result of these free-bound transitions that is responsible for the unpolarized delayed signal. This effect was observed in hydrogen and helium as well as in argon, which was the gas used throughout most of the original experiments.

Unfortunately, the experiments were not performed with this effect in mind; in fact, most of our efforts were aimed at eliminating the delayed signal in our attempts to observe Thomson scattering. As a result, the available experimental data relevant to the present work are somewhat scanty.

For the purpose of calculation, we shall consider only hydrogenic plasmas because the various cross sections and transition probabilities are well known. The results should also be fairly applicable to the $n = 3$ states of helium and the $n = 4$ states of argon which can be considered to be hydrogen-like. A level diagram of most of the He I and some of the Ar I levels is shown in Fig. VIII-4 and, as can be seen, the average quantum defect is small. Some of the argon states and the 3^3S_1 state of He I lie below $14,450 \text{ cm}^{-1}$ (1.79 ev) and therefore cannot be photo-ionized by the laser photons. This diagram was compiled from tables of Bacher and Goudsmit.⁴

Plasma parameters to be used throughout are: electron density $N_e = 2 \times 10^{13} \text{ cm}^{-3}$, electron temperature $T_e = 5 \text{ ev}$, and background gas density $N_0 = 5 \times 10^{14} \text{ cm}^{-3}$. The laser emitted a 50-joule pulse, which was 1-1.5 msec long, and the beam was focused to 2 mm in diameter in the interaction volume, which was 1 cm long. Both the

(VIII. PLASMA ELECTRONICS)

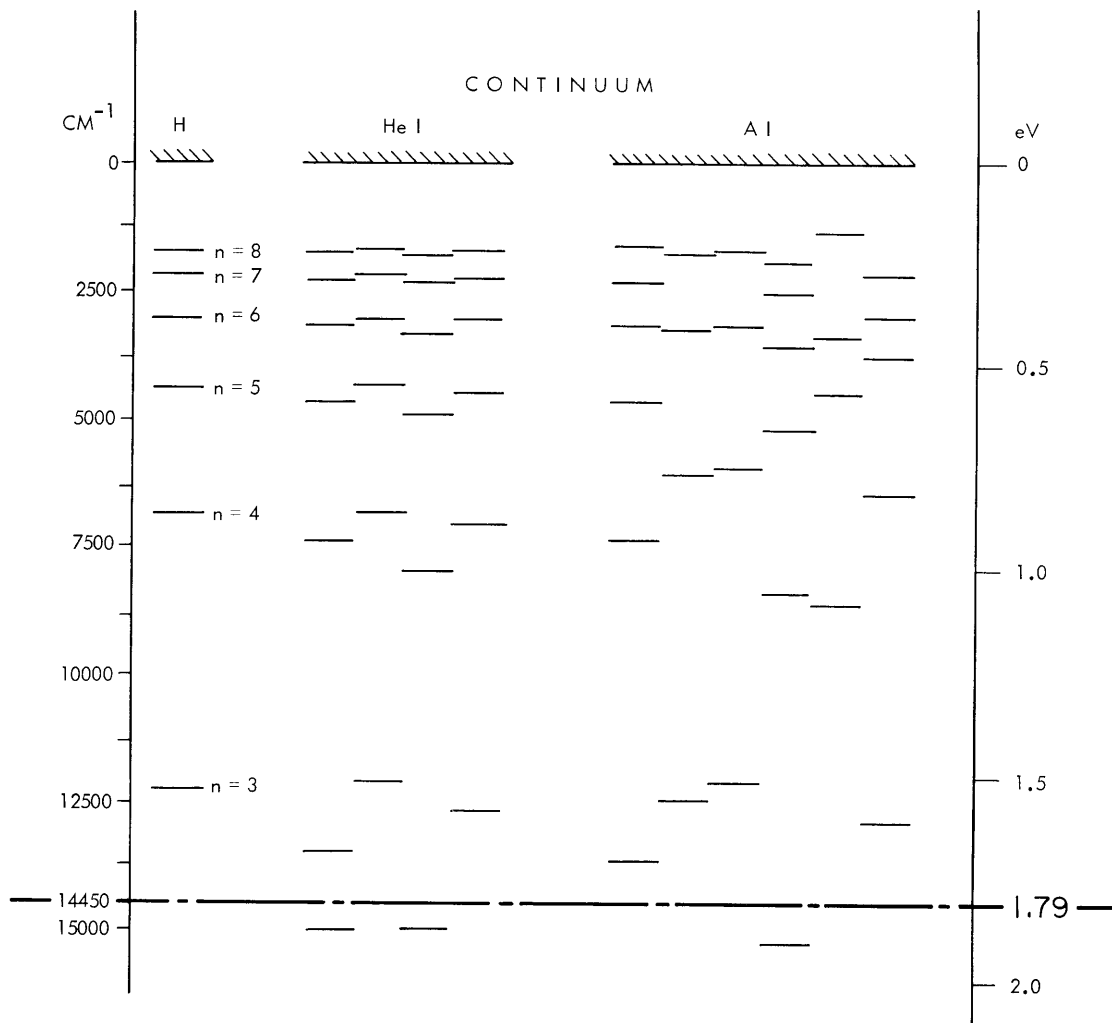


Fig. VIII-4. Partial level diagram for neutral hydrogen, helium, and argon. (Some He I and Ar I levels have been omitted for the sake of clarity.)

laser and plasma parameters could be varied, but these values are fairly typical.

The cross section for photo-ionization from a level n by radiation of frequency ν is given by

$$\sigma_{P_n}^i = \frac{1}{n^5} \left[\frac{32\pi^2 e^6 R z^4 g}{3^{3/2} h^3} \right],$$

where g is the Gaunt factor.

Because of the very strong dependence of the cross section on the initial quantum state we shall only consider the levels $n = 3$ and $n = 4$, and their behavior will dominate the processes that we suggest may take place. Even though photo-ionization of levels

with $n > 4$ is energetically possible, the cross section for $n = 5$ is down by more than an order of magnitude from $n = 3$. Ignoring the higher states will give a lower limit to the photo-ionization, but the error introduced should be small.

1. Calculation of the Densities of Excited Atoms in the $n = 3$ States

Background gas atoms are excited into the $n = 3$ state by inelastic collisions with the plasma electrons. An equilibrium population is established when the rate of excitation is balanced by spontaneous de-excitation and collisional ionization of the $n = 3$ state. Contributions to the $n = 3$ population by optical cascade transitions and electronic excitation of the $n = 2$ state are small in comparison. It is intuitively reasonable that the contribution that is due to excitation of the $n = 2$ state will be small compared with the direct excitation from the ground state because the two levels are separated by only 1.9 eV but are ≈ 10 eV above the ground state. That is, the two-collision event is much less effective than direct excitation. This can, in fact, be shown by calculation of the various processes.

The rate of excitation, S_1^3 , by collision of atoms from the $n = 1$ to the $n = 3$ state is calculated by using the work of Giovanelli⁶ and found to be

$$S_1^3 = 6.15 \times 10^{18} \text{ cm}^{-3} \text{ sec}^{-1}$$

for the given conditions. It has been assumed that each sublevel is populated according to its statistical weight.

The excited-state population is depleted predominantly by spontaneous radiative decay and collisional ionization; the rate of radiation decay is

$$S_3^{1,2} = N_3(A_{3,1} + A_{3,2}),$$

where the A's signify the average values of the transition probabilities and are defined and given by Bethe and Saltpeter.⁷ [Giovanelli does not take into account the mixing of the sublevels of the $n = 3$ state (which must take place because their separation is only 0.145 cm^{-1}) but calculates the populations of the 3s, 3p, and 3d substates separately.]

The rate of collisional ionization S_3^i of the $n = 3$ state is also calculated by Giovanelli's method⁶ and reduces to

$$S_3^i = 4.2 \times 10^7 N_3 \text{ cm}^{-3} \text{ sec}^{-1}.$$

In equilibrium, we have

$$S_1^3 = S_3^i + N_3[A_{3,1} + A_{3,2}]$$

with the result that

(VIII. PLASMA ELECTRONICS)

$$N_3 = 4.4 \times 10^{10} \text{ cm}^{-3}.$$

The validity of the foregoing calculation can be checked by comparing the density of atoms in the $n=3$ state with the value obtained from the work of McWhirter and Hearne.⁸ This more recent work gives the results of an extensive computer calculation of the density of excited states for hydrogen-like ions in a plasma. Their data are presented in the form

$$\frac{N_n}{N_n(E)} = r_0(n) + r_1(n) \frac{N_1}{N_1(E)}.$$

N_n and $N_n(E)$ are the densities and the Saha-Boltzmann population densities, respectively, of atoms in state n . They give tables of the coefficients $r_0(n)$ and $r_1(p)$ for different plasma parameters.

Using these results, we have plotted in Fig. VIII-5 the density of atoms in the $n=3$ state for different plasma parameters at a constant background pressure of 5×10^{-3} torr. These curves show that collisional ionization of the excited states depresses the excited population for $T_e > 3$ ev. Below 3 ev, the predominant loss mechanism is spontaneous de-excitation.

By interpolation, we find $N_3 = 3.5 \times 10^{10} \text{ cm}^{-3}$ for $N_e = 2 \times 10^{13} \text{ cm}^{-3}$ and $T_e = 5$ ev. This is in excellent agreement with our calculated result and the experimental work of Hinnov and Hirschberg.⁹

A similar calculation shows that the density of atoms in the $n=4$ state should be $\approx 1.5 \times 10^{10} \text{ cm}^{-3}$.

We shall continue to use the work of Giovanelli because it gives more physical insight into the competing processes that are taking place and allows us to calculate their rates but we take confidence from the close agreement with the more recent theoretical and experimental work.

2. Effect of Streaming Electrons

The core of the hollow-cathode discharge consists of a group of streaming electrons.¹⁰ If we assume that all of the arc current of 30 amps is carried by these electrons, which have an energy corresponding to the applied DC potential of 40v, then the density, N_{se} , of these streaming electrons is approximately $1.6 \times 10^{11} \text{ cm}^{-3}$. The cross section for excitation of the $n=3$ state is given⁷ as

$$\sigma_{c_1}^3 = \frac{6.2 \times 10^{-17}}{E} \text{ cm}^2 \quad \text{for } E > E_1^3$$

and

$$\sigma_{c_1}^3 = 1.55 \times 10^{-18} \text{ cm}^2 \quad \text{for } E \approx 40\text{v}.$$

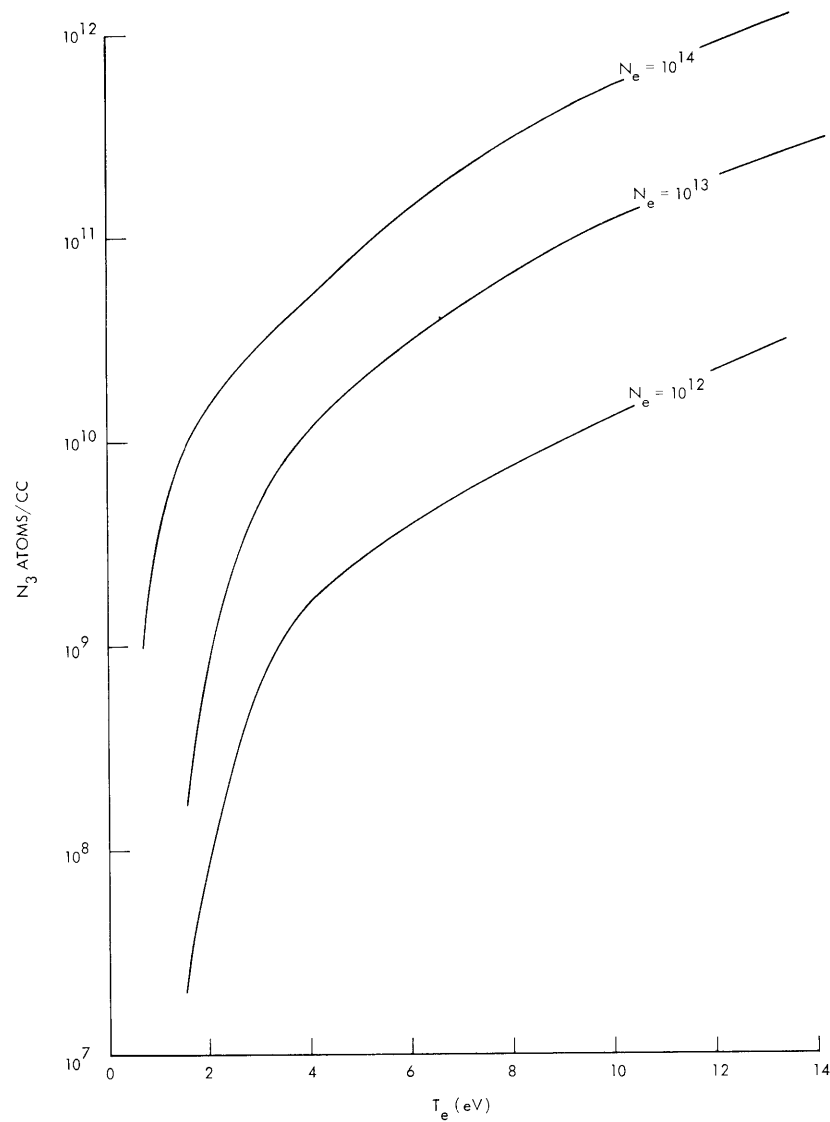


Fig. VIII-5. Population of the $n=3$ level of hydrogen as a function of electron temperature for different values of electron density. The neutral-gas density is assumed constant at $1.8 \times 10^{14} \text{ cm}^{-3}$.

This value is in order-of-magnitude agreement with the sum of the maxima of the excitation cross sections for the following levels in helium: 3^1S , 3^1P , 3^1D , 3^3P and 3^3D . These cross sections have been measured¹¹ by St. John et al., and the sum of the cross sections is $5.19 \times 10^{-18} \text{ cm}^2$.

The rate of excitation of atoms to the $n=3$ level for the given neutral density is

$$S_{c_1}^3 = N_o N_{se} \sigma_1^3 v = 1.1 \times 10^{17} \text{ cm}^3 \text{ sec}^{-1}.$$

(VIII. PLASMA ELECTRONICS)

As this rate is only 1/60 of the excitation rate by the plasma electrons, it will be ignored. We shall also neglect the excitation of the $n=4$ state by streaming electrons.

3. Photo-ionization of the Excited Neutral Atoms and Build-up of Plasma Density

The cross section for photo-ionization of various levels of hydrogen has been computed by McDowell¹² who obtained

$$\sigma_{P_3}^i = 1.2 \times 10^{-17} \text{ cm}^2$$

$$\sigma_{P_4}^i = 4 \times 10^{-18} \text{ cm}^2$$

for the photo-ionization cross section of the $n=3$ and $n=4$ levels by 1.79 eV photons. The rate of photo-ionization per unit volume of the two levels is given by

$$S_{P_3}^i = N_p N_3 \sigma_{P_3}^i c$$

and

$$S_{P_4}^i = N_p N_4 \sigma_{P_4}^i c,$$

where N_p is the photon density, and c is the velocity of light. For the given experimental conditions

$$N_p = 1.2 \times 10^{14} \text{ cm}^{-3},$$

with the result that

$$S_{P_3}^i = 1.9 \times 10^{18} \text{ cm}^{-3} \text{ sec}^{-1}.$$

Similarly, we find

$$S_{P_4}^i = 2.2 \times 10^{17} \text{ cm}^{-3} \text{ sec}^{-1}.$$

This photo-ionization increases the electron density that, in turn, gives the additional recombination radiation observed as a delayed signal. The delay is due to the fact that we must wait for the increase in electron density to cause a detectable increase in the rate of recombination. For the plasmas used, the light emission was almost 100 per cent modulated, for example, the DC level was approximately equal to the noise amplitude on the oscilloscope, and as a result, the increase in electron density had to be of the order of the steady-state electron density of $2 \times 10^{13} \text{ cm}^{-3}$ in order to give a significant delayed signal. The ambient density of excited atoms (≈ 3 or $4 \times 10^{10} \text{ cm}^{-3}$) is

much too low to result in an appreciable build-up of electron density during the laser pulse, so we must now consider the replenishment of the interaction region with excited neutrals.

The number of neutrals N'_0 that enter the interaction volume of surface area $A \text{ cm}^2$ during the laser pulse which lasts for τ sec is given by

$$N'_0 = \frac{1}{4} N_0 v_0 A \tau,$$

with the result that

$$N'_0 = 10^{16} \text{ atoms}$$

for the given conditions.

In order to compute the fraction of these neutrals which is excited and then photo-ionized, we need to know the lifetimes that the atoms have for the various processes that can take place. These processes and the lifetimes are listed in Table VIII-1. The fraction $F_{\text{ex}_1}^3$ of the neutrals excited to $n=3$ is given by

$$F_{\text{ex}_1}^3 = \frac{1}{\tau_{c_1}^3} \left[\frac{1}{\tau_{c_1}^2} + \frac{1}{\tau_{c_1}^3} + \frac{1}{\tau_{c_1}^4} + \frac{1}{\tau_{c_1}^i} \right]^{-1} = 7.7 \times 10^{-2}.$$

Similarly, the fraction excited to $n=4$ is $F_{\text{ex}_1}^4 = 2.2 \times 10^{-2}$.

The atoms only spend $\approx 1 \mu\text{sec}$ in the interaction volume, and hence the number excited in this region is

$$N_3 = 7.7 \times 10^{-2} \frac{10^{-6}}{3 \times 10^{-5}} 10^{16} = 2.6 \times 10^{13} \text{ atoms.}$$

Of these, a fraction $F_{p_3}^i$ is photo-ionized, where

$$F_{p_3}^i = \frac{1}{\tau_{p_3}^i} \left[\frac{1}{\tau_{c_3}^i} + \frac{1}{\tau_{R_3}^{1,2}} + \frac{1}{\tau_{p_3}^i} \right]^{-1} = 0.24.$$

For the $n=4$ state, we obtain

$$F_{p_4}^i = 0.09.$$

Therefore the number of atoms photo-ionized during the laser pulse is 8.5×10^{12} .

Depopulation of a level by photo-ionization will, of course, result in a decrease in the number of radiative transitions from that level and hence in a decrease in the

(VIII. PLASMA ELECTRONICS)

Table VIII-1. Lifetimes of various atomic processes taking place in the plasma.

Process	Lifetime
Collisional excitation $n=1 \rightarrow n=2$	$\tau_{c_1}^2 = 3.7 \mu\text{sec}$
Collisional excitation $n=1 \rightarrow n=3$	$\tau_{c_1}^3 = 29 \mu\text{sec}$
Collisional excitation $n=1 \rightarrow n=4$	$\tau_{c_1}^4 = 100 \mu\text{sec}$
Collisional ionization $n=1 \rightarrow n=\infty$	$\tau_{c_1}^i = 7.6 \mu\text{sec}$
Collisional ionization $n=3 \rightarrow n=\infty$	$\tau_{c_3}^i = 2.4 \times 10^{-8} \text{ sec}$
Collisional ionization $n=4 \rightarrow n=\infty$	$\tau_{c_4}^i = 8.3 \times 10^{-9} \text{ sec}$
Radiative decay $n=3 \rightarrow n=1,2$	$\tau_{R_3}^{1,2} = 1.02 \times 10^{-8} \text{ sec}$
Radiative decay $n=4 \rightarrow n=1,2,3$	$\tau_{R_4}^{1,2,3} = 3.25 \times 10^{-8} \text{ sec}$
Photo-ionization $n=3 \rightarrow n=\infty$	$\tau_{P_3}^i = 2.3 \times 10^{-8} \text{ sec}$
Photo-ionization $n=4 \rightarrow n=\infty$	$\tau_{P_4}^i = 7 \times 10^{-8} \text{ sec}$

corresponding spectral line intensity. The intensity of the H_α line in a discharge similar to the one used in the original experiment has been observed to decrease by approximately 3 per cent during the laser pulse,¹³ which fact is in agreement with the calculation above.

If now we assume that the ions resulting from the photo-ionization process stay in the interaction region of volume V , the increase in electron density would be

$$\Delta n_e = \frac{8.5 \times 10^{12}}{V} = 2.7 \times 10^{14} \text{ electrons cm}^{-3}.$$

This increase in electron density is comparable to that estimated from the amplitude of the delayed signal if we assume that the light output arises from electron-ion radiative recombination (proportional to N_e^2) and also use the known steady-state electron density. An absolute intensity measurement of the delayed signal obtained from a hydrogen plasma, together with the known recombination coefficient plus reasonable estimates of the recombination continuum spectrum,¹⁴ yielded $N_e \approx 10^{14} \text{ cm}^{-3}$.

The argument depends critically upon the assumption that the plasma produced by photo-ionization does not rapidly leave the interaction region. The properties of the excess plasma will now be considered. We shall begin with the temperature of the ions produced by photo-ionization; this temperature initially will be the same as the neutral-gas temperature. The following consideration of ion-neutral and electron-ion scattering shows that the ions and neutral atoms are, in fact, very closely coupled.

We consider a case in which the ions are at 1 ev. This value is much too large, as we shall see, but it is the lowest value to which we can make a reasonable extrapolation from available experimental data. The total scattering cross section for A^+ on A is $\approx 10^{-14}$ cm² at 1 ev¹⁵ and represents the sum of the elastic scattering and charge-transfer cross sections. This cross section results in an ion-neutral collision frequency $\nu_{i0} = 2 \times 10^5$ sec⁻¹. The rate of energy transfer from the electron to the ions is calculated by using the result given¹⁶ by Rose:

$$\frac{du_i}{dt} = \frac{e^4 n_e m_e \ln \Lambda \left[1 - \frac{2u_i}{3kT_e} \right]}{2\pi \epsilon_0^2 (2\pi m_e kT_e)^{1/2} m_i \left[1 + \frac{4}{3\pi} \left(\frac{m_e u_i}{m_i kT_e} \right)^{3/2} \right]}.$$

For the case under consideration, we can assume that both terms in square brackets equal unity and then this expression yields the maximum value of du_i/dt . In equilibrium we have

$$\frac{du_i}{dt} = \nu_{i0} (T_i - T_0)$$

from which we find

$$T_i - T_0 = 5.5 \times 10^{-2} \text{ ev},$$

where T_i and T_0 are the ion and neutral atom temperatures.

This is an upper limit to the temperature difference. Because the neutrals will be fairly close to room temperature, the ion energy will be < 1 ev and therefore ν_{i0} will be even higher, since σ_{i0} is rising rapidly at these low energies. It would appear, therefore, that it is perfectly reasonable to assume that we can replace the neutral-gas atoms in the observation region with ions formed by photo-ionization which will be at the same temperature as the plasma ions. Cold electrons are also formed and will be heated to the temperature of the background plasma electrons (5 ev) in a time that is of the order of $\tau_{\theta ee}$, the time for scattering through 90°, where

(VIII. PLASMA ELECTRONICS)

$$\tau_{\theta_{ee}} = \frac{25.8 \pi m_e \epsilon_0^2 (kT_e)^{3/2}}{e^4 N_e \ln \Lambda} \approx 4 \times 10^{-8} \text{ sec.}$$

The plasma so formed will leave at a rate governed by its ambipolar diffusion coefficient.

4. Decay of Excess Plasma Density

The excess plasma density produced in the interaction volume can decay by diffusion, recombination or a combination of both.

We first consider the ambipolar-diffusion coefficient D_a given by

$$D_a = \frac{D_+ \mu_- + D_- \mu_+}{\mu_+ + \mu_-}.$$

Here D and μ are the diffusion coefficients and mobilities, and the subscripts refer to the ions and electrons. The quantities D and μ are related by the Einstein relation,

$$\frac{D}{\mu} = \frac{kT}{e}.$$

The value of μ can be calculated by means of

$$\mu = \frac{e}{m \nu_m},$$

where ν_m is the collision frequency for momentum transfer. For the case of T_+ and T_e ,

$$D_a \cong \frac{kT_e}{e} \mu_+.$$

The value of μ_+ has been experimentally determined¹⁷ and found to be $2.35 \times 10^5 \text{ cm}^2 \text{ volt}^{-1} \text{ sec}^{-1}$ at $N_o = 5 \times 10^{14} \text{ cm}^{-3}$, with the result that

$$D_a = 1.2 \times 10^6 \text{ cm}^2 \text{ sec}^{-1}.$$

Using this value of D_a , we can calculate the diffusion length Λ given by

$$\Lambda^2 = D_a t,$$

where t is the observed characteristic time of the anomalous signal which we take to be 10^{-3} sec . The value of Λ thus obtained is $\Lambda = 35 \text{ cm}$ and this value implies that there can be no local increase in plasma density, but that the excess plasma uniformly distributes itself throughout the whole of the ambient plasma column.

An obvious difficulty now appears. If the excess plasma density is $\approx 10^{14} \text{ cm}^{-3}$, and if according to the diffusion calculation this density exists throughout the whole plasma column, where did all the excess particles come from? It is highly improbable that the excess density is a direct result of an interaction between neutral particles and the laser. This can be shown by the following calculation.

The number of excess particles, N_{excess} , required to fill the plasma column corresponds to a density of 10^{14} cm^{-3} and is given by the product of the excess density and the plasma volume. For our apparatus, the plasma volume was $\approx 40 \text{ cm}^3$ (1 cm in diameter, 50 cm long), and hence we need $N_{\text{excess}} = 4 \times 10^{15}$ particles.

If all of these particles are to come from a laser interaction, they must necessarily enter the laser beam, and an upper limit to the number that can do this during the laser pulse is 10^{16} . Hence we see that if we are to make 4×10^{15} ions from the 10^{16} neutrals, we need the inordinately high efficiency of 40 per cent.

The diffusion calculation contradicts the qualitative observation that the delayed signal was localized to a small region near the laser beam. Note that if the excess plasma rapidly diffuses away from the interaction region, the delayed signal, if it is due to recombination radiation, should be observed throughout the whole plasma column.

As it is difficult to find any fault in the diffusion calculation, a firm resolution of the problem awaits further careful measurements, both of the spatial distribution of the signal and the true value of the excess density.

5. General Discussion and Proposed Experiments

Although, at first sight, it would appear that to observe Thomson scattering, a high degree of ionization is necessary so that the delayed signal can be avoided, these delayed signals will not be observed if a "Q-spoiled" laser is used, for the reason that the short pulse length of 10^{-8} sec does not afford sufficient time for the excited-state population and its accompanying increase in ion density by photo-ionization to significantly perturb the steady-state electron density. Also, some discrimination of a Thomson-scattering signal against the delayed signal may be attained by taking advantage of the polarization of the Thomson signal.

Several experiments have been devised to test this theory, and the proposed apparatus is shown in Fig. VIII-6. The system is basically the one used originally, except for the addition of differential pumping in order to attain a high degree of ionization. By feeding gas into the observation chamber, the degree of ionization may be varied without altering the plasma source conditions. The optical detection system is also shown and includes a dichroic mirror to enable us to monitor the radiation from the interaction volume by two detectors simultaneously. This system will permit the following experiments to be made.

(VIII. PLASMA ELECTRONICS)

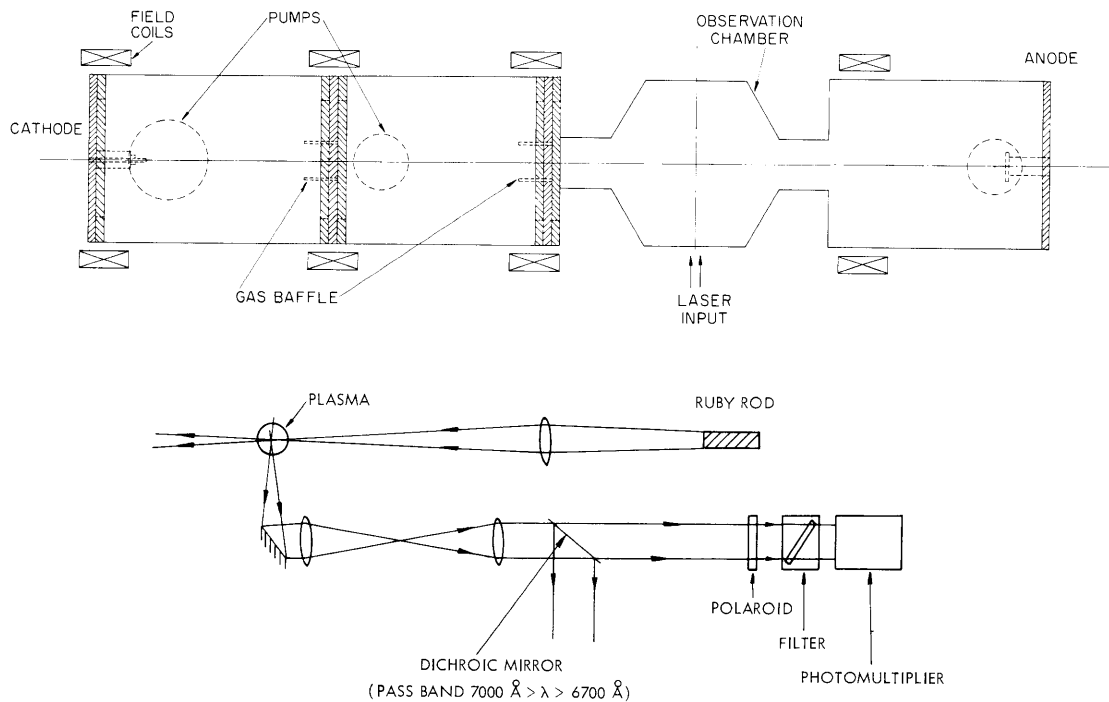


Fig. VIII-6. Schematic diagram of the proposed experiment, including the cross section of the optical system.

(i) Monitoring the H_{α} line of 6563 \AA which results from the transition $n=3$ to $n=2$ in order to observe the change in the population of atoms in the $n=3$ state. The intensity of the H_{α} line should decrease as the $n=3$ population is depleted by photo-ionization.

(ii) Monitoring the delayed signal as a function of wavelength across one of the Balmer edges will enable us to confirm that the radiation is due to free-bound transitions.

(iii) An attempt will be made to place a probe close to the interaction region in order to measure the increase in electron density.

Other experiments include quantitative measurements of the delayed signals as a function of neutral-gas pressure and laser power.

E. Thompson

References

1. L. M. Lidsky, D. J. Rose, and E. Thompson, Quarterly Progress Report No. 73, Research Laboratory of Electronics, M. I. T., April 15, 1964, pp. 98-105.
2. E. Thompson and G. Fiocco, Quarterly Progress Report No. 69, Research Laboratory of Electronics, M. I. T., April 15, 1963, pp. 74-80.
3. D. J. Rose, L. M. Lidsky, and E. Thompson, Radiation enhancement in an optical Thomson-scattering experiment, Bull. Am. Phys. Soc. 9, 323 (1964).

4. R. F. Bacher and S. Goudsmit, Atomic Energy States (McGraw-Hill Book Company, New York, 1932).
5. R. W. Ditchburn and V. Öpik, Atomic and Molecular Processes, edited by D. R. Bates (Academic Press, Inc., New York, 1962), p. 86.
6. R. G. Giovanelli, Australian J. Sci. Res. A1, 275, 289 (1948).
7. H. Bethe and R. Saltpeter, Handbuch der Physik, Vol. XXXV, edited by S. Flügge (Springer-Verlag, Berlin, 1957), p. 352.
8. R. W. P. McWhirter and A. G. Hearne, Proc. Phys. Soc. (London) 82, 641 (1963).
9. E. Hinnov and J. G. Hirschberg, Phys. Rev. 125, 795 (1962).
10. L. M. Lidsky, S. D. Rothleder, D. J. Rose, and S. Yoshikawa, J. Appl. Phys. 33, 2490 (1962).
11. R. M. St. John, F. L. Miller, and C. C. Lin, Phys. Rev. 134, A888 (1964).
12. M. R. C. McDowell, Report ORNL-347, Thermonuclear Semi-Annual Progress Report for period ending April 30, 1963, p. 64.
13. E. T. Gerry, Private communication, Research Laboratory of Electronics, M. I. T., 1964.
14. M. J. Seaton, Rep. Progr. Phys. 23, 313 (1960).
15. W. H. Cramer, J. Chem. Phys. 30, 641 (1959).
16. D. J. Rose, and M. Clark, Jr., Plasmas and Controlled Fusion (The M. I. T. Press, Cambridge, Mass., and John Wiley and Sons, Inc., New York, 1961), p. 165 ff.
17. E. W. McDaniel, Collision Phenomena in Ionized Gases (John Wiley and Sons, Inc., New York, 1964), p. 466.

E. THOMSON SCATTERING FROM A HOLLOW-CATHODE ARC PLASMA*

A new experimental facility has been constructed to investigate the use of Thomson scattering as a plasma diagnostic method. Preliminary results of a similar experiment were first reported by Thompson and Fiocco.¹ The present experiment was designed to be a detailed study of both the incoherent (electron Doppler-broadened) and coherent scattering of a ruby laser beam from a hollow-cathode arc plasma.

Consider the scattering of an incident light beam of wave vector $|\vec{K}_1| = \frac{2\pi}{\lambda}$ through an angle θ (see Fig. VIII-7). The magnitude of the vector $\vec{\Delta K}$, $(|\vec{\Delta K}| = \sqrt{2} |\vec{K}_1| \sqrt{1 - \cos \theta})$ is the quantity of interest. $1/|\vec{\Delta K}|$ is, effectively, the length in the plasma over which the amplitudes of radiation scattered by individual electrons add coherently. We define: $\alpha = \frac{1}{|\vec{\Delta K}| \lambda_D}$, where λ_D is the Debye length. Then, for $\alpha \ll 1$, the coherence length is less than a Debye length, and on this scale the electron motion is completely random, so that the scattered wavelength distribution reflects only the Doppler shifts caused by

* This work was supported in part by the U. S. Atomic Energy Commission (Contract AT(30-1)-3221).

(VIII. PLASMA ELECTRONICS)

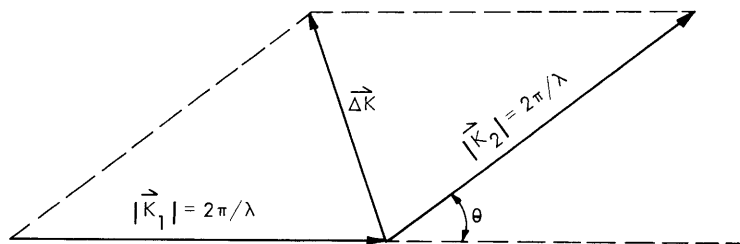


Fig. VIII-7. Scattering of incident light beam of wave vector $|\mathbf{K}| = 2\pi/\lambda$.

the random electron velocities, and no coherent effects enter. The wavelength distribution of the scattered radiation yields essentially the electron velocity distribution. For $\alpha > 1$, however, $\frac{1}{|\Delta\mathbf{K}|}$ is larger than a Debye length, and collective motions of the plasma electrons become important. This problem has been treated theoretically by Salpeter² for essentially equilibrium cases, and by Rosenbluth and Rostocker³ for certain nonequilibrium situations. For large α , the result is primarily that the incident radiation is broadened by the ion temperature, and satellites appear at plus and minus the frequency of plasma oscillations of wavelength $\frac{2\pi}{|\Delta\mathbf{K}|}$, the shape of the satellites being dependent on α . A discussion of the spectrum of scattered radiation that would be expected from several typical laboratory plasmas has been prepared.⁴

The hollow-cathode arc yields plasmas with electron densities of from 10^{13} to 10^{14} and with electron temperatures of 1-4 volts. For the ruby-laser wavelength (6934 \AA) under these conditions, α may be varied from approximately 4 to 0.05 by varying the scattering angle from 2° to 90° .

The present experimental arrangement allows scattering at 45° (small α) and at various small angles from 2° to 10° (large α). Thus far, experiments have been carried out only at 45° . The design of the 45° system is similar to that used by Thompson and Fiocco¹ in their 90° scattering experiment. A similar plasma source has been described by Lidsky et al.⁵ The addition of a hollow anode with a small amount of gas fed through it seemed to improve the performance of the arc, and this modification was employed in the experiments reported here. Langmuir-probe measurements of the argon plasma indicated an electron density of 5×10^{13} in a region 1 cm in diameter around the center of the arc. The measured electron temperature was 4 volts, but this measurement is questionable because the high value of ion saturation current limited the measurements to the tail of the electron distribution. The background pressure in the scattering chamber was 2×10^{-4} torr with an argon arc.

The scattering apparatus was calibrated by using Rayleigh scattering from a known density of nitrogen. This procedure allows the direct calibration of the entire apparatus

without having to account individually for all of the solid-angle, filter-attenuation, and photomultiplier gain factors. By integrating the Thomson-scattered spectrum over wavelength and by comparing this signal with the signal obtained for Rayleigh scattering, one obtains a direct measure of the electron density. The analysis of the scattered spectrum was made by rotating a 3 \AA bandwidth filter.

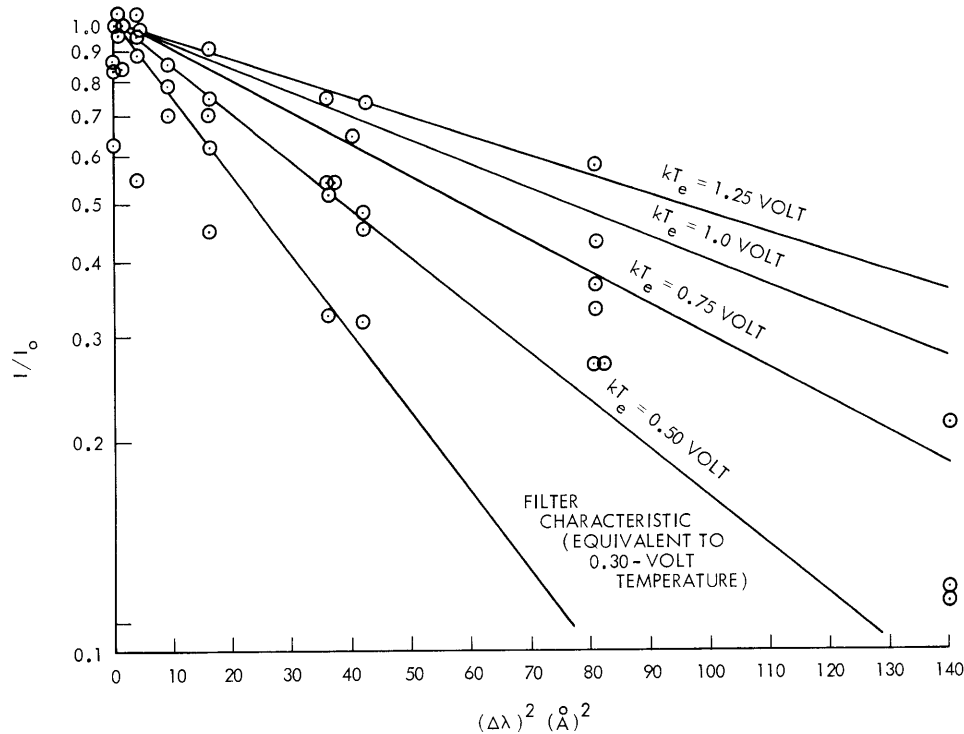


Fig. VIII-8. Plot of preliminary results.

Preliminary data are presented in Fig. VIII-8 and exhibit much scatter, primarily because of fluctuations in the background plasma light level and changes in laser alignment during the experiment. The logarithm of the scattered signal amplitude is plotted against the wavelength shift in angstroms squared. For a Maxwellian electron velocity distribution, the result should be a straight line. Several lines are shown for various temperatures. The wing transmission characteristic of the filter, obtained by Rayleigh scattering, is also shown for comparison.

As a result of the scatter of the data, the electron temperature cannot be accurately determined, but it appears to lie between 0.5 ev and 1 ev. This is in strong disagreement with the probe data, which indicated 4 volts. The probe, however, was measuring the tail of the electron distribution, while the Thomson scattering was measuring the

(VIII. PLASMA ELECTRONICS)

main body of the distribution function. Comparison of the magnitude of the scattered signal with Rayleigh scattering yields an electron density of approximately 5×10^{13} , in good agreement with the ion saturation probe measurements. We do not obtain the signals observed by Thompson and Fiocco¹ at large wavelength displacement from the laser line. They attributed these effects to the ionization and excitation of the neutral background by the laser pulse. The neutral background was kept very low in our experiments by the use of high pumping speed in the scattering chamber; this procedure leads to a highly effective degree of ionization.

E. T. Gerry

References

1. E. Thompson and G. Fiocco, Scattering of light from (plasma) electrons III, Quarterly Progress Report No. 69, Research Laboratory of Electronics, M.I.T., April 15, 1963, pp. 74-80.
2. E. E. Salpeter, Phys. Rev. 120, 1528 (1960); 122, 1663 (1961).
3. M. N. Rosenbluth and N. Rostoker, Phys. Fluids 5, 776 (1961).
4. E. Gerry and R. Patrick, Thomson scattering computations for laboratory plasmas (submitted to Phys. Fluids as a research note).
5. L. M. Lidsky, S. D. Rothleder, D. J. Rose, S. Yoshikawa, C. Michelson, and R. J. Mackin, Jr., J. Appl. Phys. 33, 2490-2497 (1962).